Micro-nanosystems for electrical metrology and precision instrumentation

A. Bounouh[1], F. Blard[1,2], H. Camon[2], D. Bélières[1], F. Ziadé[1]

[1]LNE – 29 avenue Roger Hennequin, 78197 Trappes, France, alexandre.bounouh@lne.fr
[2]LAAS/CNRS – Université de Toulouse - av du colonel Roche, 31077 Toulouse cedex 4, France

Abstract: This paper present results of work undertaken for exploring MEMS capabilities to fabricate AC voltage references for electrical metrology and high precision instrumentation through the mechanical-electrical coupling in MEMS devices. Several first devices have been designed and fabricated using a Silicon On Insulator (SOI) Surface Micromachining process. The measured MEMS AC voltage reference values have been found to be from 5 V to 100 V in a good agreement with the calculated values performed with Coventor and Comsol finite elements software. These tests structures have been used to develop the read-out electronics to drive the MEMS and to design new devices with improved characteristics.

Keywords: MEMS, AC voltage, Pull-in effect, SOI.

1. INTRODUCTION

From MEMS devices made up of membranes, beams or seesaw structures, several applications in electrical metrology are possible as AC and DC voltage references, RF-DC converters, current reference, low frequency voltage divider and RF and microwaves power sensors [1-3]. Such devices are made of micro-machined electrodes of which one at least is movable thanks to the application of an electrostatic force between the two electrodes, inversely proportional to the square of the gap. For voltage references, one uses the pull-in effect of a electro-mechanical microsystem having a movable electrode (Fig.1)

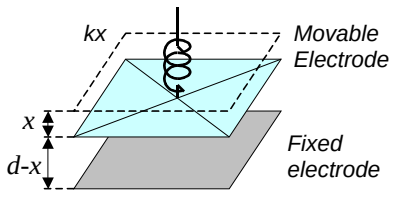

Fig. 1. MEMS with variable capacitor

The stable displacement x of the movable electrode is limited to the third of the gap named d. In the characteristic voltage-displacement, the pull-in voltage V_{pi} corresponds to the maximum voltage applied to the capacitive MEMS beyond which the two electrodes are put in contact. However, if the previous structure is now biased with an AC sinusoidal current of amplitude I_{RMS} and frequency ω, the AC voltage presents, according to the current I_{RMS}, a maximum:

$$V_{AC}^{max} = V_{pi} = \sqrt{8kd^2 / 27C_0} \qquad (1)$$

where C_0 is the capacitance at x = 0 and *k* the spring constant (Fig.2).

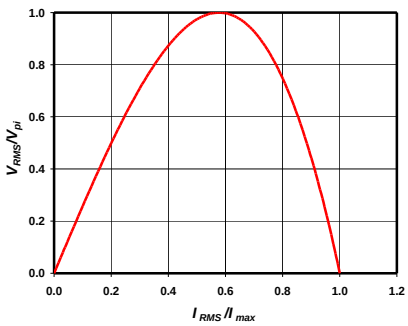

Fig. 2. MEMS Voltage versus I_{RMS} biasing current

This point can be used as a stable AC voltage reference since its relative variation in this point depends only on the square of that of the current:

$$\Delta V_{RMS}/V_{pi} \sim -3/2\ (\Delta I/I_{max})^2 \qquad (2)$$

In order to have the required stability for primary and secondary metrology fields and precision instrumentation (some parts in 10^7 per year), special designs and architectures featuring low sensitivity with respect to strain and geometrical dispersion have to be investigated, as well as technological processes featuring low residual stress and high repeatability.

2. DESIGN AND FABRICATION OF TEST DEVICES

The first set of MEMS structures were based on a silicon disk plate featuring different configuration of the suspending springs to ensure a controlled piston mode motion. The structures have been designed using a Coventor and Comsol softwares. Fig.3 shows the layouts of the movable part of the structures that have been designed and used for the tests. The first device (1) is a 500 µm-radius disk plate with three curved 1300 µm-long springs of 10 µm width. Device (2) is very similar to (1)

design and has the same dimensions, only the curved part of the springs in (2) are attached together forming a ring of 10 µm width, which slightly increases the stiffness of the structure and then V_{pi}. The aim of this design is to improve the vertical guidance of the movable plate. The same disk plate as previously (r =500 µm) is used for forming the last design (3) having four straight springs (360 µm × 10 µm).

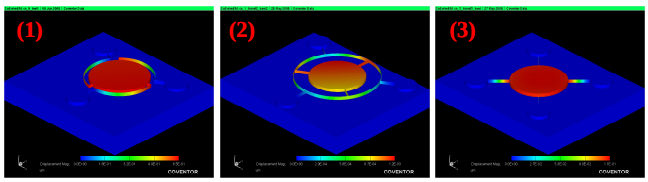

Fig. 3. MEMS test structures.

The MEMS have been fabricated with TRONIC's process available as a process foundry through the Multi Project Wafer. It consists of a Silicon On Insulator (SOI) surface micromachining process. The SOI top layer is a 60 µm thick monocrystalline silicon layer used for the mechanically active layer, exhibiting excellent mechanical characteristics (it can tolerate up to 10^{10} cycles without any crack or fatigue [4]). The silicon dioxide layer acting as insulator and spacer defines the gap of 2 µm height and the silicon substrate features 450 µm thick acting as the fixed electrode. Silicon wafers resistivity is in the range of 0.02 Ω.cm obtained by a high boron p-type doping of 2.10^{18} cm^{-3}.
To ensure the stability of the MEMS, a vacuum hermetic silicon wafer level packaging protects the die. The final structure is composed by the assembly of the SOI wafer where the MEMS is realized and a silicon wafer acting as a cap for protecting the MEMS. The non-sealed areas are defined by partial etch of a silicon dioxide initially realized and the metallization define the sealing areas for assembly. After assembly, via holes are realized to allow electrical contact to pads.
The previous layouts have been used for elaborating the MEMS structures. Fig.4 shows photos of the three fabricated MEMS. Let us note that on the same die there are 3 MEMS hermetically packaged and 3 other MEMS in a no hermetic packaging. This configuration makes it possible to assess the packaging effect on the stability of the AC voltage references.

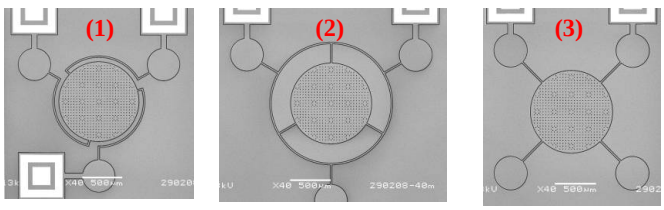

Fig. 4. MPW MEMS structures fabrication

.

3. MEASUREMENT RESULTS

The multi-physics characterization platform has been set up in order to verify the model parameters and to perform the appropriate characterization to determine the stability coefficient of the MEMS based AC voltage. First C-V curves have been carried out on the MEMS of structure (1) by using a RLC-meter. An external DC bias voltage was applied to the MEMS and the capacitance was measured with an AC voltage of 0.1 V at a frequency of 100 kHz.

As shown in Fig.5, the MEMS exhibits a pull-in effect at V_{pi} = 1.9 V. However, another mechanical state corresponding to V_{pi}=4.5 V can also be observed. This last point is to be compared to the calculated value of 5.26 V.

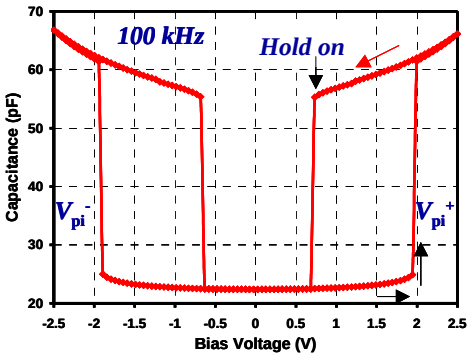

Fig. 5. C-V characteristic of the MEMS of structure (1) at 100 kHz signal frequency

To drive the MEMS to the pull-in voltage for defining the ac voltage reference, we have developed the read-out electronics of Fig.6. As the MEMS have to be biased with an AC current, it is used in the feedback loop of the A1 amplifier consisting in a voltage-to-current converter. The amplifier A1 should have a great product gain-bandwidth to work up to some hundreds kHz. However, this kind of components has not small voltage offset and polarisation current, this is why we use a low frequency precision amplifier A2 to fix the DC out-put voltage at zero. Figure 6 shows the frequency response of both amplifiers A1 and A2, which make this electronics usable in the range 10 kHz –1 MHz.

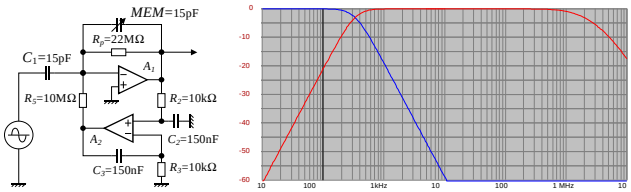

Fig. 6. Voltage-to-current read-out electronics

Measurements of the MEMS out-put RMS voltage in function of the current I_{RMS} flowing in the MEMS (U-I curve) have been carried out at frequencies ranging from 10 kHz to 200 kHz. Fig.7 displays the characteristics MEMS out-put voltage of structure (1) versus the current I_{RMS} at 100 kHz. All curves show the same maximum of the out-put voltage corresponding exactly to the pull-in voltage *V*pi = 1.9 V observed in the C-V curves.

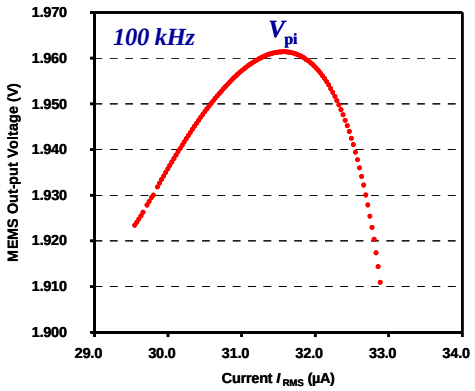

Fig. 7. U-I curve of MEMS (1) at 100 kHz

4. DESIGN AND FABRICATION OF ENHANCED DEVICES

New MEMS structures have been designed with the aim to get samples showing lower pull-in voltages for the best performance of the read-out electronics. Indeed, as the MEMS capacitor is used in the feedback loop of the A1 amplifier consisting in a voltage-to-current converter, this amplifier should have a great product gain-bandwidth to work up to some hundreds kHz. In this case, the most powerful amplifiers have voltage supply about ±15 V at most. Two structures were targeted to have pull-in voltages of 5 V and 10 V. The layout of the design is depicted in Fig.8 and it is the same for both MEMS. It is based on a silicon disk plate with straight suspending springs. The 5 V device is a 1105 µm-radius disk plate with three 1072 µm-long springs of 10 µm width. 10 V device has the same diameter of the movable plate with 884 µm length of the springs. Both structures are guarded by a 65 µm width silicon ring to avoid the effect of any leakage currents. The improvement carried out in these new structures concern the effective capacitance of the movable part, which becomes much higher than the parasitic capacitance. Indeed, the value of the movable capacitance is now of 22 pF.

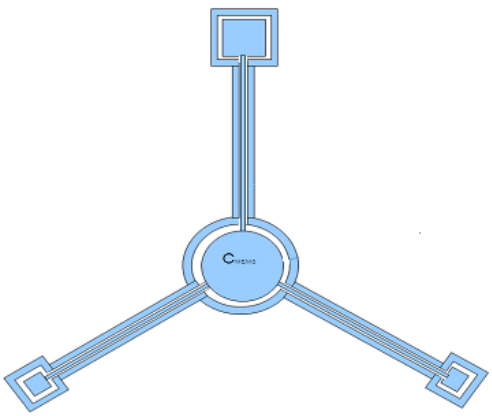

Fig. 8. Layout of the enhanced MEMS

The design of the structures is carried out following 3 steps: *i*) definition of deposit type, etching and thickness of the layers; *ii*) drawing of the masks; *iii*) Mesh of the different regions. The calculations have been performed with the electromechanical formulation of Coventor software. For each structure, the displacement *x* of the movable electrode is calculated by varying the DC voltage applied between the movable electrode and the silicon substrate. Fig.9 shows for the 10 V structure the simulations and the calculated displacement according to the DC voltage, which gives a simulated pull-in voltage at x=0.66 µm corresponding to 1/3 of the gap of 2 µm defined by the thickness of the SOI silicon dioxide.

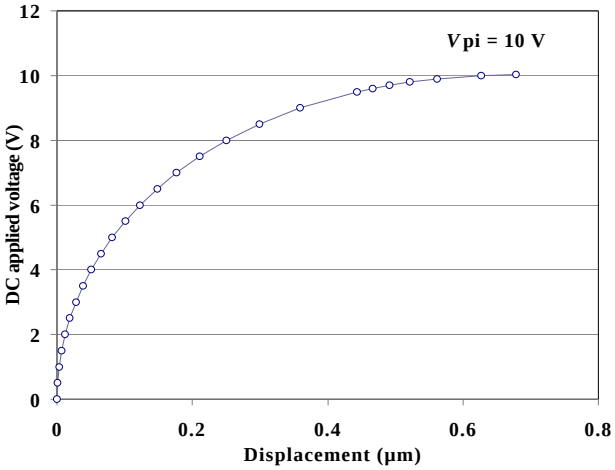

Fig. 9. Coventor modelling of 10 V structure and pull-in voltage calculation.

The calculated parameters of the two structures are summarized in table 1 where the capacitance C_0 at x=0, the spring constant *k*, the resonance frequency and the pull-in voltage are given.

Table 1. Calculated characteristics of the new structures

Structures	C_0 (pF)	k (N/m)	f_0 (kHz)	V_{pi} (V)
5 V	22.8	1437	10	5.5
10 V	22.8	437	18	10

The MEMS have been fabricated with TRONIC's process with the Silicon On Insulator (SOI) surface micromachining process previously used for the test structures. Each fabricated die contains the two types of MEMS (5 V and 10 V) and a vacuum hermetic silicon wafer level packaging has been used to protect the die. However, we have also fabricated structures where the packaging is not hermetic to compare both systems and to evaluate the effect of the environmental conditions.

Fig.10 shows a photo of the two fabricated MEMS, which are on the same die there. For each MEMS, we have contact pads corresponding to the movable electrode, the guard, the silicon cap protecting the die and the silicon substrate. Let us note that for the hermetic die, the pads are larger and contribute more in the effective capacitance of the MEMS.

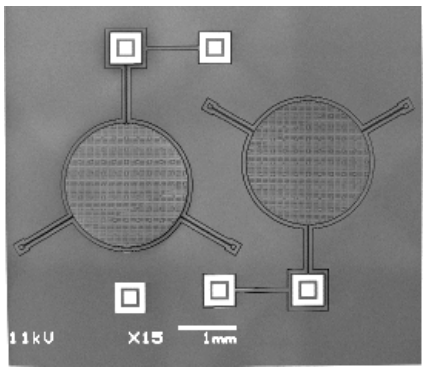

Fig. 10. Photo of the 5V and 10V MEMS structures

Deep Level Transient Spectroscopy (DLTS) measurements have been carried out on these MEMS to analyze the dynamic behaviour of the movable plate by measuring the capacitance change in time.

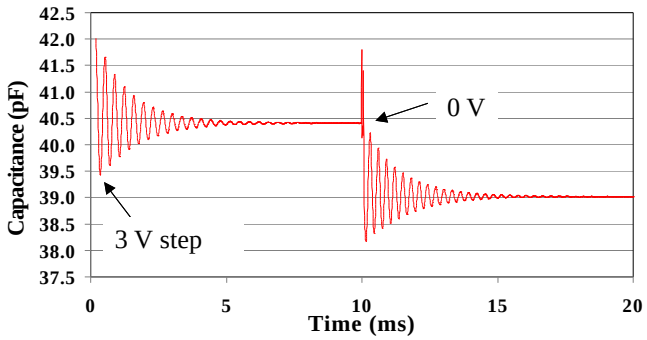

Fig. 11. 5V MEMS capacitance versus time showing the response of the structure to a voltage step of 3 V.

Fig.13 represents the response of the 5V MEMS of the die named HP11 to a DC voltage step of 3 V during 10 ms. The membrane oscillations represented by the oscillations of the MEMS capacitance are clearly observed over a time period lower than 5 ms beyond which the movable electrode becomes stable. Moreover, the membrane behaves in the same way when establishing and stopping the voltage step. This indicates that the system is not very damped since the MEMS in HP11 die are hermetically sealed in a vacuum. The resonance frequency of the MEMS determined from the DLTS measurements is of 2.8 kHz to be compared to the expected value of 10 kHz for this structure.

Two other hermetic samples named HK6, HK11and one no hermetic named NH15 have been used for the first C-V and U-I measurements. Fig.12 presents a C-V curve for the HK11 sample where the 5 V MEMS has been tested.
It exhibits a pull-in voltage around 4 V, which is lower than the calculated value of 5.5 V. The same value is obtained for all the other dies (hermetic and no hermetic). For the 10 V MEMS, the pull-in effect occurs at 7 V, which is once again lower than the expected value of 10 V. The slight difference between the measured and calculated values indicates that there is a more important buckling of the movable membrane than expected.

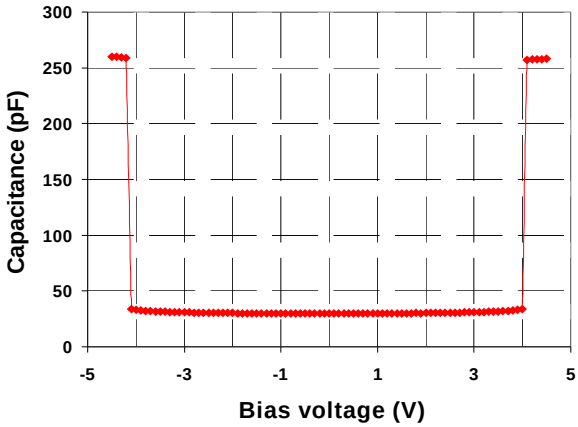

Fig. 12. C-V curve of the 5V MEMS (HK11) at 100 kHz signal frequency

The U-I curves corresponding to the MEMS out-put RMS voltage in function of the current I_{RMS} flowing in the MEMS have been carried out at a frequency of 100 kHz. Fig.13 displays this characteristic for the 5V MEMS of the HK11 die. The maximum of the out-put voltage corresponds at approximately 4.1 V, which is exactly the value of the pull-in voltage *V*pi observed in the C-V curves.

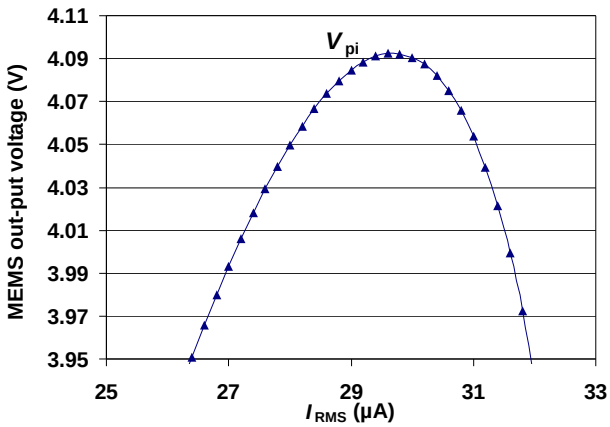

Fig. 13. U-I curve of the 5 V MEMS (HK11) at 100 kHz

4. CONCLUSION

The stability of the AC reference voltage corresponding to the maximum of these curves is under test by using a specific read-out electronics based on the amplitude modulation of the main biasing ac signal. The results will be presented at the time of the conference as well as the assessment of the whole MEMS fabrication. The results of this assessment will be used to validate the models, to understand the dispersions and to propose consolidated architectures more robust with respect to the dispersion in the MEMS fabrication.

REFERENCES

[1] B.P. van Drieënhuizen, “Integrated Electrostatic RMS to Converter”, Thesis, 1996.

[2] M. Suhonen et al, “AC and DC Voltage Standards Based on Silicon Micromechanics, CPEM98, pp. 23-24, 1998.

[3] EMMA project report, Information Societies Technology, IST200028261EMMA, 2005.

[4] H. Camon, C. Ganibal, “Advantages of alternative actuating signal for MEMS actuators”, Sensors & Actuators A136 N°1, pp.299-303, 2007.R. Abraham, J. E. Marsden, T. Ratiu, Manifolds, Tensor Analysis, and Applications. 2 ed. New York, Springer-Verlag, 1988.